

Polyamidoamine Dendrimer Modified Silica Nanoparticles: A Promising Sorbent for Benzoylurea Insecticides Detection in Tea Infusions

Yanchao Zhang,^a Xiaoyan Cui,^a Xiwen Lin,^a Yiduo Mi,^a Yumei Yan,^a Xiaoyang Liu,^a
Keren Jiao,^a Haixiang Gao,^a Runhua Lu^a and Wenfeng Zhou[✉]*,^a

^aDepartment of Applied Chemistry, College of Science, China Agricultural University, 100193 Haidian District, Beijing, China

This research aims to develop a precise and efficient dispersive solid-phase microextraction (DSPE) technique using third-generation polyamidoamine (PAMAM) dendrimer-grafted nanoparticles to quantify benzoylurea pesticides in green tea, black tea, and oolong tea infusions. The extraction efficiency is optimized through single-factor adjustments of key parameters, including adsorbent quantity (5-20 mg), adsorption duration (5-20 min), desorbent identity (methanol, acetonitrile), volume (100-600 μL), sodium chloride concentration (0-10%, m/v), and sample solution pH (3-8). The optimized method demonstrates linearity in the range of 2-500 $\mu\text{g L}^{-1}$, with limits of detection (LODs) ranging from 0.6-1.5 $\mu\text{g L}^{-1}$ and limits of quantification (LOQs) from 2.0-5.0 $\mu\text{g L}^{-1}$. Recovery rates of 81.2-96.0% are achieved, with intra-day relative standard deviations (RSDs) of 1.4-2.8% and inter-day relative standard deviations of 2.0-3.9%, indicating high accuracy and repeatability. The successful application of detecting residues in commercial tea samples underscores the strong potential of the technique to determine benzoylurea analyte levels.

Keywords: polyamidoamine dendrimer, silica nanoparticles, dispersive solid-phase extraction (DSPE), benzoylurea insecticides, tea infusion samples

Introduction

Benzoylurea insecticides, innovative insect growth regulators that emerged in the 1970s, disrupt the molting and feeding processes of the insects during the larval stage by blocking or inhibiting chitin synthesis.¹ Their outstanding properties, including high insecticidal activity, moderate environmental persistence, broad insecticidal spectrum, and low mammalian toxicity, have popularized their use for pest prevention.^{2,3} However, excessive use may lead to deposit accumulation, posing risks to human health through chronic exposure, long-term toxic effects and bioaccumulation in food chains.⁴ Some benzoylurea insecticides, such as diflubenzuron and flufenoxuron, are considered compounds with a risk of causing chronic effects.⁵ Hence, developing a rapid, simple, and sensitive analytical technique to monitor benzoylurea insecticides is crucial.

Green tea constitutes a substantial share of 20-22% of the global market. It is renowned for its distinctive

properties and potential health benefits, including reducing blood pressure and mitigating cardiovascular disease risk.⁶⁻⁹ However, the increasing demand for this beverage has raised concerns regarding pesticide residues, leading to the establishment of stringent maximum residue limits for benzoylurea insecticides in tea in many countries. To illustrate, Japan has defined specific limits for chlorfluazuron, diflubenzuron, flufenoxuron, hexaflumuron, teflubenzuron, and triflumuron in tea at 10, 20, 15, 15, 20, and 0.02 mg kg⁻¹, respectively.⁵ While some studies⁴ have examined benzoylurea insecticide residues in oolong tea, limited attention has been given to the identification of diverse benzoylurea insecticides in green tea.

As an indispensable preprocessing step in most analytical workflows, the meticulous handling of biological and environmental samples through selective treatment, isolation, matrix component removal, and analyte enrichment is imperative.¹⁰ Despite the prevalence of classical techniques, such as liquid-liquid extraction (LLE) and solid-phase extraction (SPE) remain widely employed despite their tedious protocols, extensive labor requirements, and dependence on substantial volumes of hazardous organic solvents.^{11,12} Over the past 20 years, Green

*e-mail: zhouwenfeng@cau.edu.cn

Editor handled this article: Andrea R. Chaves (Associate)



Analytical Chemistry (GAC) has been firmly established in analytical methods to reduce energy consumption and hazardous chemicals and minimize waste.¹³ Recent environmental consciousness has spurred the adoption of alternative, eco-friendly methods, including dispersive-, micro-, stir bar-, and magnetic solid-phase extraction methods, as well as thin film and in-tube microextraction methods.¹⁴⁻¹⁷ Among these alternatives, dispersive solid phase extraction (DSPE) stands out by refining and enhancing traditional SPE through streamlined, rapid procedures and reduced solvent consumption, amplifying extraction efficiency and analyte enrichment.^{17,18}

Since the extraction materials serve as the critical separation medium, extensive research has been done on DSPE enhancement via advanced sorbents like multi-walled carbon nanotubes (MWCNTs), metal-organic frameworks (MOFs), and graphene.¹⁹ Dendrimers have also attracted attention as ideal 3D adsorbents conferring uniformity and porosity. Polyamidoamine (PAMAM), as one of the earliest well-studied dendrimers, has been widely applied in various fields, including drug delivery and membrane science, given its configurable surface groups surrounding an internal cavity that enable host-guest capture of analytes.^{20,21} Typically, dendrimers comprise a central core, numerous branched units, and abundant surface groups.^{22,23} The selectivity improvements of the PAMAMs may arise from tailoring its functionalization to target analytes of interest. Insoluble supports, such as silica, could mitigate material losses and facilitate analyte recovery.²⁴⁻²⁶ Shirani *et al.*²⁷ also used SiO₂ to prepare Fe₃O₄@SiO₂ nanocomposites, which were combined with deep eutectic solvent (marine acid: cumarine) and used as adsorbents for the detection of tetracycline residues in food samples, and achieved remarkable results. However, realizing the combined potential of selective PAMAM modifications and optimized recovery remains an open research avenue.

This study presents a dispersive solid phase microextraction (DSPE) approach using PAMAM grafted silica nanoparticles to select benzoylurea insecticides from complex tea infusion matrices. Extraction efficiency optimization entails modulating sorbent amounts, contact time, pH, and ionic strength. The morphology of synthesized sorbent is confirmed through analytical characterization. Applying high-performance liquid chromatography to real-world tea beverage and infusion samples with diode array detection (HPLC-DAD) demonstrates appreciable analyte enrichment and improved detection sensitivities. While primarily emphasizing DSPE optimization, further exploration in tailoring the SiO₂/PAMAM nanocomposite selectivity could enable more targeted and efficient extractions.

Experimental

Chemicals and reagents

Pesticide standards, such as hexaflumuron, lufenuron, flufenoxuron, and chlorfluazuron, and other chemicals, 3-aminopropyltriethoxysilane (NH₂-(CH₂)₃-Si-(OC₂H₅)₃, APTES) and methyl acrylate were purchased from Aladdin Reagent Co., Ltd. (Shanghai, China). Ethylenediamine, tetraethyl orthosilicate (TEOS), methanol, ethanol, sodium chloride (NaCl), ammonia, and sodium hydroxide (NaOH) were obtained from Sinopharm Chemical Reagent Co., Ltd. (Beijing, China).

Instruments and analytical conditions

An Agilent 1100 HPLC (high-performance liquid chromatography) system was used in this study, equipped with a diode array detector (DAD) and an auto sampler, all controlled via an Agilent workstation. Analytes were using a Spursil C18 column (5 μm, 4.6 × 250 mm, Dikma Limited) at a column temperature of 30 °C. The mobile phase for gradient elution comprised an acetonitrile and water mixture (0-0.4 min, 70:30, v/v; 3-17 min, 52:48, v/v; 17-35 min, 67:33, v/v; 35-37 min, 70:30, v/v) and the flow rate was maintained at 1 mL min⁻¹. The detection wavelength was 220 nm, and the sample injection volume was 10 μL.

The surface morphology of the SiO₂/PAMAM composite was examined using a scanning electron microscope (SEM, model S-3400N, manufactured by Hitachi, Tokyo, Japan) at an accelerating voltage of 15 kV. Additionally, a transmission electron microscope (TEM, model JSM-2100F, JEOL, Tokyo, Japan) was utilized at an operating voltage of 200 kV. Infrared spectra were obtained using a Fourier transform infrared spectrometer (FTIR, Spectrum 100, PerkinElmer, Waltham, Massachusetts, USA). The spectral acquisition was performed in the range of 4000 to 400 cm⁻¹ with a resolution of 4 cm⁻¹.

Preparation of tea infusion samples

The tea drink was purchased from a local market. Two commercial tea samples, green tea and oolong tea, were acquired online. The infusion sample preparation involved steeping 5.0 g of each tea in 250 mL of boiling water for 5 min. Sample preparation adhered to the Chinese National Standard Methodology²⁸ for the sensory evaluation of tea. The beverage and infusions were carefully sieved and refrigerated at 0 °C.

Synthesis of SiO₂/PAMAM-G3 nanocomposite

Synthesis of SiO₂

Silicon dioxide (SiO₂) was prepared mixing 10 mL of ammonium hydroxide, 100 mL of ethanol and 3.6 mL of deionized water and stirring for 2 min. Next, 5.84 g of TEOS were added to the mixture and stirred for 3 h at room temperature. The resulting SiO₂ particles were purified through five cycles of washing with ethanol and then dried under vacuum at 60 °C.

Synthesis of SiO₂-NH₂

Aminopropyl-grafted silica (SiO₂-NH₂) was prepared by dispersing 2.5 g of SiO₂ nanoparticles in 75 mL of ethanol under 30 min ultrasonication. After adding 20 mL of triethylamine, the mixture was stirred for 2 h at 40 °C, then mixed dropwise with 20 mL of ethanol-dissolved (APTES) and stirred for another 12 h. The final SiO₂-NH₂ product was carefully washed thrice with acetone, isolated by centrifugation, and dried under a vacuum at 60 °C for 12 h.

Synthesis of SiO₂/PAMAM-G3 nanocomposite

SiO₂/PAMAM nanoparticles were synthesized through Michael addition and amination reactions. Michael addition is a nucleophilic addition of a carbanion to an α,β -unsaturated carbonyl compound, while amination involves introducing an amine group. These reactions started from SiO₂-NH₂. Specifically, 1 g of SiO₂-NH₂ nanoparticles were dispersed in 20 mL of methanol and

sonicated for 30 min. Then, 20 mL of methyl acrylate were added to the mixture under ice bath conditions and stirred for 15 h.²⁹ The resultant product, SiO₂/PAMAM-G0.5, was washed with methanol five times, resuspended in 10 mL of methanol, and ultrasonicated for 30 min. Under ice bath cooling, 2 mL of ethylenediamine were added dropwise, and the mixture was stirred for 3 h at 35 °C. The product, SiO₂/PAMAM-G1, was washed 5 times with methanol and dried under vacuum for 12 h. Higher-generation dendrimer-bound SiO₂ nanoparticles were synthesized by repeating the Michael addition and amination reactions (Figure 1a).

Dispersive solid phase extraction (DSPE) procedure

The DSPE procedure is illustrated in Figure 1b. This DSPE method represents an essential sample clean-up and concentration step before instrumental analysis for the selective extraction of trace benzoylurea insecticides from complex tea infusion matrices. Briefly, 30 mg of SiO₂-PAMAM were added to 8 mL of aqueous sample. Preliminary trials demonstrated this as the optimal sorbent quantity for maximizing extraction efficiency while minimizing matrix interferences. This quantity efficiently captured the spiked analytes from a relatively large sample volume. The suspension was vortexed for 2 min to thoroughly disperse the sorbent particles and ensure adequate contact between the sorbent surface and the target analytes, partitioning into the miniature extraction phase. Upon attaining adsorption equilibrium

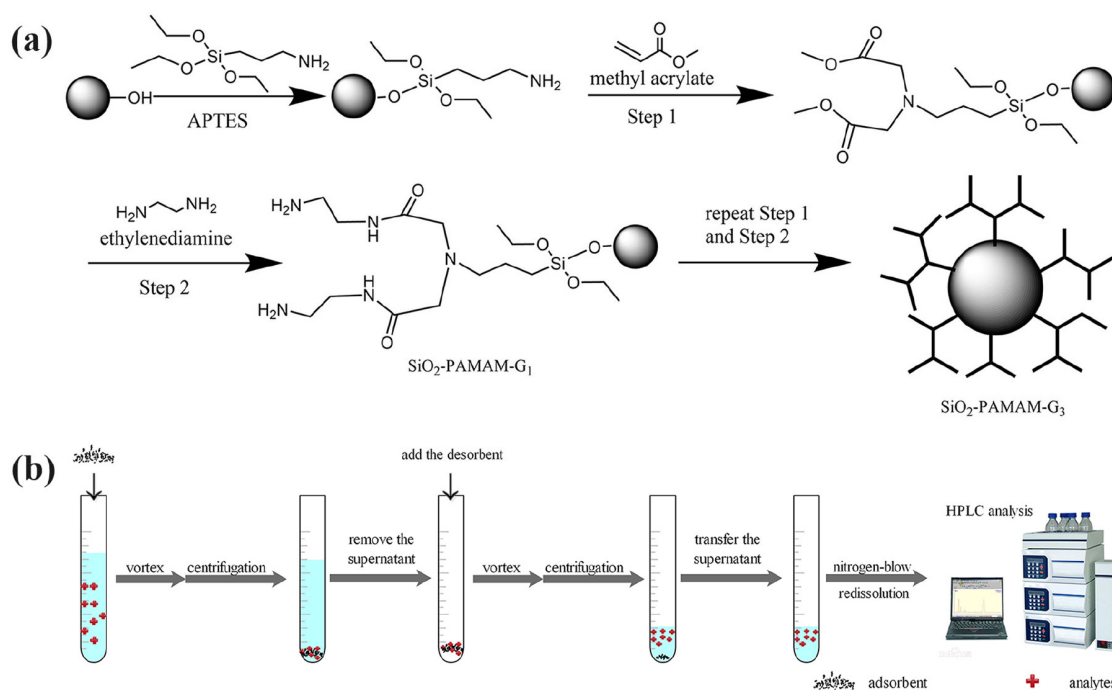


Figure 1. Schematic of (a) the synthesis of SiO₂/PAMAM-G3, and (b) the dispersive solid phase extraction (DSPE) procedure.

after sufficient contact time, the mixture was centrifuged at 5000 rpm for 3 min, accomplishing rapid and efficient phase separation. After carefully discarding the supernatant, a gentle stream of ultra-high pure (UHP) nitrogen gas was used to remove any residual moisture on the collected sorbent to prevent degradation or losses. Next, 2.25 mL of chromatographic grade ethyl acetate was introduced as the desorption solvent and vortexed for 1 min to facilitate the rapid and thorough interphase mass transfer. This desorption solvent was selected owing to strong extraction recoveries based on analyte properties. Following phase separation via centrifugation, the ethyl acetate extract containing the concentrated insecticides was transferred to another tube for the solvent evaporation step. The samples were finally reconstituted in 100 μ L of HPLC grade acetonitrile. The extracted procedure was completed in 30 s to enable downstream chromatographic analysis with high preconcentration factors up to 80 \times .

Results and Discussion

SiO₂/PAMAM-G3 nanocomposite characterization

Understanding the interactions between SiO₂/PAMAM-G3 sorbent and flufenoxuron is crucial as it provides insights into the extraction process and the dynamics between the sorbent and analyte in DSPE. FTIR spectroscopy was used to analyze the nanocomposite and its interaction with the insecticide. Figure 2a illustrates the successful grafting of PAMAM dendrimers onto SiO₂ nanoparticles, confirmed by the N–H stretching vibration of amine groups at 3367 cm⁻¹. Peaks at 1645 and 1546 cm⁻¹ are also observed, corresponding to C=O stretching and N–H bending vibrations, respectively. After adsorbing flufenoxuron, noticeable shifts are observed in all three peaks to 3363, 1641 and 1535 cm⁻¹

for N–H stretching, C=O stretching and N–H bending modes, respectively. These changes suggest hydrogen bonding interactions between the dendrimer and the analyte molecule. Understanding this binding affirms flufenoxuron extraction through hydrogen bonding. Recent research^{30,31} has given more support to the importance of hydrogen bonding for pesticide-dendrimer interaction. The interactions between pesticides and different nanomaterials, including hydroxylated fullerenes (fullerenols), were studied by Geitner *et al.*³⁰ using discrete molecular dynamics (DMD) simulations. They discovered that fullerenols with moderate hydroxylation showed the highest binding to pesticide molecules via hydrogen bonding and hydrophobic interactions, which aligns well with our observations. Likewise, Zhou *et al.*³¹ prepared magnetic PAMAM dendrimers for the extraction of organochlorine pesticides from water samples and demonstrated the importance of hydrogen bonding in the adsorption process through DMD simulations. These studies examined different nanomaterials and pesticides, but their results strongly confirm our interpretation of the FTIR peak shifts and the role of hydrogen bonding in the SiO₂/PAMAM-G3 and flufenoxuron interaction. Nevertheless, further studies are required to distinguish between the particular interaction mechanisms. It also provides insights into the role of different PAMAM peripheral groups in adsorption, thus enhancing our understanding of sorbent sorbate dynamics to optimize DSPE performance.

The SEM image shows roughly spherical particles with some surface roughness, which could potentially indicate the presence of a PAMAM coating (Figure 2b). Comparative TEM image between the unmodified silica and SiO₂/PAMAM-G3 confirms the effective grafting of dendrimer coatings onto SiO₂ nanoparticle surfaces (Figure 3). The electron microscopy findings directly

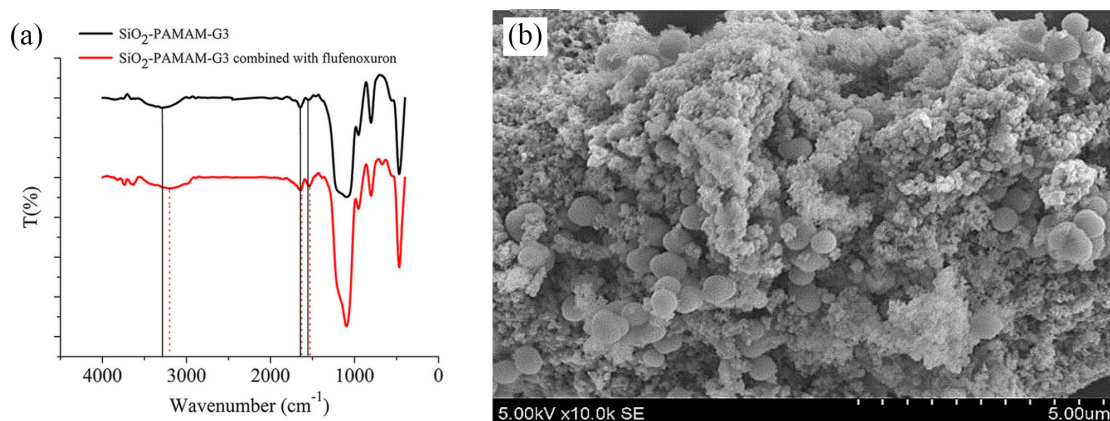


Figure 2. (a) FTIR (KBr) spectra of SiO₂/PAMAM-G3 and the compound of SiO₂/PAMAM-G3 and flufenoxuron, (b) scanning electron microscopy (SEM) images of SiO₂/PAMAM-G3.

corroborated the FTIR spectral evidence, verifying the successful preparation of dendrimer-functionalized SiO₂ nanocomposites.

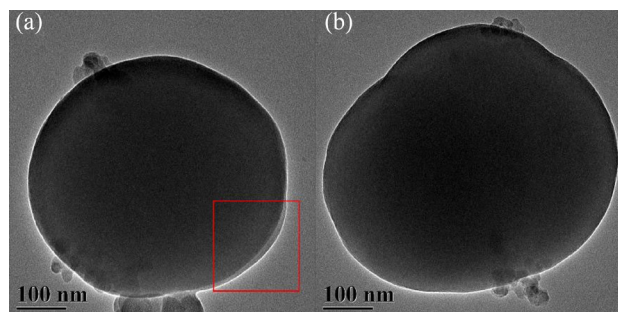


Figure 3. Transmission electron microscopy (TEM) images of (a) SiO₂/PAMAM-G3 and (b) bare SiO₂.

Optimization of DSPE methodology

Several extraction parameters were optimized via single-factor analysis to enhance DSPE efficiencies, such as sorbent selection and quantity, adsorption duration, and desorbent properties. Stringently controlling these conditions is imperative towards balancing challenges around sorbent stability and analyte affinity. Oolong tea infusions were used as the model matrix in all optimization trials. Each experiment was performed in triplicate for statistical robustness.

Adsorption conditions affecting the extraction performance of SiO₂/PAMAM-G3

Nanocomposite

To assess the impacts of adsorption conditions on the extraction performance of the developed DSPE method, we systematically compared the efficacy of SiO₂ functionalized with PAMAM across generations G1, G2, and G3 to unmodified SiO₂ nanoparticles. These materials were strategically selected based on our hypothesis that the increasing functional group density in higher generation PAMAM dendrimers would correlate with enhanced analyte adsorption capability provided by their precisely engineered branched structures. The quantitative recoveries of four model benzoylurea insecticides (hexaflumuron, lufenuron, flufenoxuron, and chlorfluzuron) are examined across the sorbent variations. Recoveries increased progressively with higher-generation PAMAM dendrimers, with SiO₂/PAMAM-G3 nanocomposites demonstrating higher extraction efficiencies (Figure 4a). This trend can be attributed to the larger surface amine groups and the larger interior void volumes in higher-generation dendrimers. This enables cooperative improvements in sorbent-analyte

complementary chemical and structural interactions such as intermolecular hydrogen bonding. These findings showcase the excellent promise of deliberately designed dendrimeric nanostructures for advanced and selective analyte extractions, an active area of innovation in separation science engineering.

The effects of different amounts of SiO₂/PAMAM-G3 nanocomposite sorbent on extraction efficiency were investigated. Quantities of the tailored dendrimer nanomaterial were varied to assess its ability to capture and enrich insecticide analytes in model solutions. As shown in Figure 4b, the recovery rates of all four benzoylurea analytes increased with the increase in SiO₂/PAMAM-G3 levels from 0 to 30 mg. This improvement can be attributed to the greater total surface area and functional groups available for hydrogen bonding interactions with target insecticides. However, further increases in quantities decreased the recoveries, possibly due to a decline in the uniformity and consistency of nanoparticle dispersions during adsorption and desorption steps caused by viscosity effects. Therefore, the accessibility to sorbent interaction sites decreased. A 30 mg sorbent dosage was selected for subsequent DSPE experiments to balance the extraction efficiency and ensure practical dispersion stability. These investigations provide insights into the mechanisms governing sorbent adsorption capabilities.

These results suggest that SiO₂/PAMAM-G3 offers unparalleled extraction capabilities under optimal conditions. FTIR spectra substantiating PAMAM grafting onto SiO₂ nanoparticles explain its remarkable performance. When flubenzuron is adsorbed, noticeable N–H peak redshifts signify hydrogen bonding underpinning extraction. SEM and TEM further verify successful dendrimer immobilization on SiO₂, with microscopy unveiling SiO₂ encapsulation by a coarse polymer layer following PAMAM conjugation. These characterizations highlight SiO₂/PAMAM-G3 nanocomposites as highly promising sorbents for solid-phase extraction.

Achieving adsorption equilibrium, defined as the uniform interfacial distribution of analytes between the synthesized nanosorbent and complex tea extract, is a time-dependent process underpinned by sufficient sorbent-matrix contact induced by vortex mixing. However, excessive vortex durations confer no additional extraction benefits as equilibrium plateaus. Therefore, extraction time optimization is imperative. Quantitative examination reveals a steady enhancement in extraction efficiency over 30–150 s of vortexing (Figure 4c). Notably, the rise tapered off beyond 120 s as analyte adsorption reached saturation. Considering no appreciable benefit manifested with further vortexing, whereas duration linearly increases,

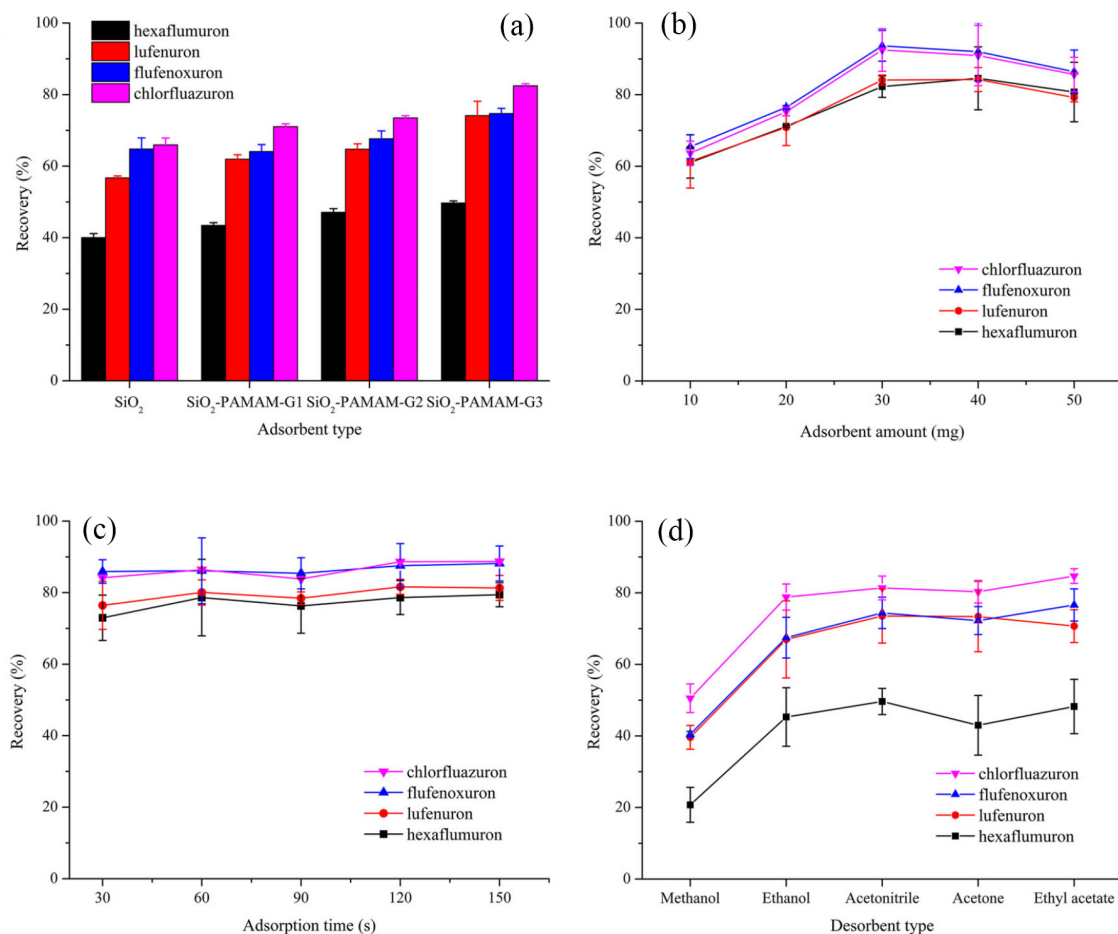


Figure 4. Effect of (a) adsorbent type, (b) amount of adsorbent, (c) vortex time for adsorption and (d) desorbent type on the extraction efficiency.

120 s enables equilibrium attainment judiciously and time-efficiently.

Impact of desorption conditions on recovery efficiency

Initial optimization of solvent volume: to determine the optimal conditions for eluting benzoylurea insecticides from the adsorbent SiO₂/PAMAM-G3 with the help of methanol, acetonitrile, and ethyl acetate applied in a systematic way at different volumes. At 5 mL volume, the recovery was the highest of 92% by acetonitrile and 91% by ethyl acetate, while by methanol it was 89%. This can be explained by the good water miscibility of acetonitrile that allows the analyte to be dissolved efficiently and the intermediate polarity of acetonitrile that promotes desorption over adhesion to the solid surface (Figure 4c).

Further optimization of ethyl acetate volume: after the primary screening, further optimization focused on ethyl acetate because of its lower toxicity and cost.³² By adjusting the volume of ethyl acetate to 2.25 mL, a positive impact on the recovery of 94% was observed. This phase of optimization emphasizes the need to harmonize solvent effectiveness with ecological and safety issues.

Systematic examination of solvent efficiency: we also carried out a general assessment of solvents such as methanol, ethanol, acetonitrile, acetone, and ethyl acetate in terms of their recovery percentages and green chemistry metrics. Recoveries from ethyl acetate were always very high, reaching up to 92%, that was higher than the 85% recovery with acetonitrile and much better than recoveries from other solvents. Ethyl acetate probably works here because of its intermediate polarity that makes it able to solubilize pesticides effectively and prevents interaction with the sorbent.

Calibrating desorbent volume for environmental sustainability: the calibration of the desorbent volume minimizes unnecessary organic solvents waste and maintains extraction efficiency. As shown in Figure 5a, 2.25 mL of ethyl acetate furnishes peak recovery, which therefore will be the best candidate for further experiments. Ethyl acetate shows good miscibility and dispersion kinetics. However, the quest for alternative greener solvents remains critical, which highlights our mission to improve environmental sustainability.^{33,34}

Optimizing contact time for efficient desorption:

adequate pesticide-desorbent exchange involves an ideal contact time that enables elution of the analyte, while additional vortexing enhances the sorbent dispersion. The optimization of different contact times (Figure 5b) indicates that 60 s is the optimum desorption time, whereas decreasing recoveries may be attributed to re-adsorption of the analyte. This approach gives a pattern for environmental, food safety, and pharmaceutical applications where economic desorption is required. Despite these promising results, applying this methodology to complex samples requires further validation.

Impact of NaCl concentration and pH

The NaCl concentration in the sample solution impacts not only the solubility of other substances but also the viscosity of the solution.³⁵ By increasing the NaCl percentage while keeping all factors constant, we found that an optimal concentration of 8% (m/v) offers the highest recovery rates (92%) compared to lower concentrations of sodium chloride, resulting in recoveries between 82 and 87%, as shown in Figure 5c. This is due to the salting out phenomenon, where higher levels of ions

disrupt the hydration layers surrounding solute particles, effectively concentrating them within the phase. However, once the NaCl concentration exceeds 10%, increased viscosity between molecules hinders mass transfer rates, considerably decreasing recoveries despite solubility.

The pH of the solution impacts not only the interaction between the pesticide and the adsorbent, but also the extraction capacity and existence form of the adsorbent.^{36,37} It also affects ionization equilibria, hydrogen bonding and hydrophobic interactions, ultimately influencing their affinities. Initially, pH changes reduce hydrophobicity and weaken sorbent affinities for certain pesticides due to their pK_a values. Recoveries peaked at pH 6.0 and 8.0, as shown in Figure 5d. Recovery declined under alkaline conditions, suggesting that base-catalyzed hydrolysis may degrade labile components. It is considered optimal since a pH of 6.0 already provides recovery rates in our experiments without any additional adjustments. Further investigations involving classes of pesticides could provide more insights into pH-affecting sorption mechanisms. Since non-halogenated pesticides persisted across a pH range, it indicates potential opportunities for selective optimization.

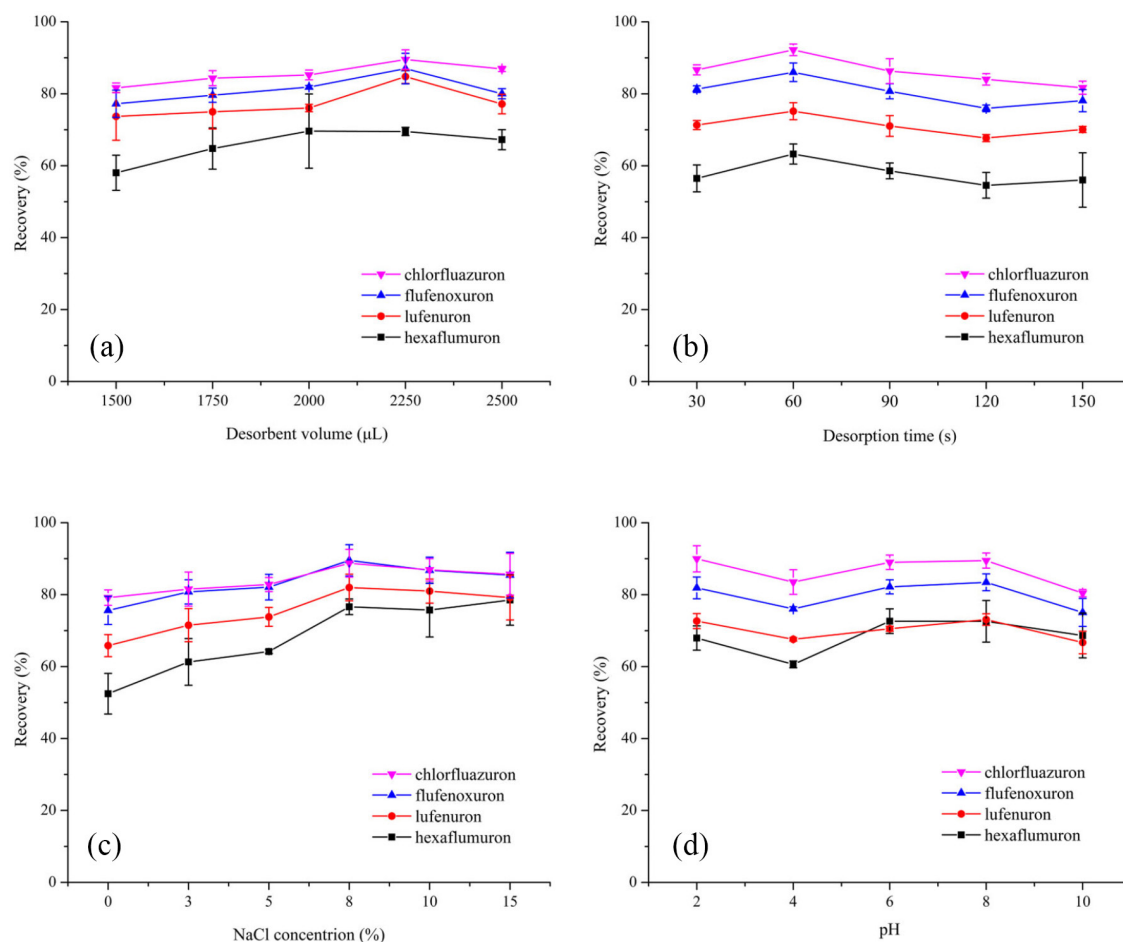


Figure 5. Effect of (a) volume of desorbent, (b) vortex time for the desorption, (c) NaCl concentration and (d) pH on the extraction efficiency.

Secondly, the interplay between NaCl concentration and pH adjustment are important issues for setting up the best extraction conditions. The ionization state of the analyte ions and sorbent can be disturbed if the concentration of NaCl is too high because it can alter the ionic strength of the solution and this influences the ionization state of both the analytes and the sorbent. The revision of this element influences the electrostatic interactions that are important for efficient adsorption and desorption processes. Taking into account the effect of interactions, it becomes mandatory to adjust pH levels in order to maintain the analyte in the best state for getting out of the processing. Among those factors, the existence of a large number of interactions within a matrix may significantly influence the analyte behavior; this explains why the maintenance of a high extraction efficiency and consistency is of paramount importance, especially when dealing with complex samples.

Although this methodology shows promise, extensive validation of its application for diverse sample types is important. This validation should focus on assessing the effectiveness of recovery and identifying the limitations of its applicability in environmental, pharmaceutical, and food analyses.

Method validation

Post-optimization, the DSPE methodology is assessed by examining sensitivity, linearity, accuracy and precision. Tea specimens were spiked with four benzoylurea insecticides across graded concentrations to characterize their performance (Table 1). Broad linear calibration ranges were obtained (2-500 or 5-500 $\mu\text{g L}^{-1}$) with correlation coefficients of 0.9994-0.9998. Appreciable recovery percentages (81.2-96.0%) were also achieved, affirming the accuracy of the method.

To determine reliability and reproducibility, intra-day relative standard deviation (intra-RSD) was calculated using five replicates at three spiked levels (50, 100 and 200 $\mu\text{g L}^{-1}$), realizing 1.4-2.8% values, demonstrating consistency across different concentrations (Table 2). Inter-

day relative standard deviation (inter-RSD) was evaluated by repeating the protocol over five days at 100 $\mu\text{g L}^{-1}$ in triplicates, furnishing 2.0-3.9% values, which confirms the stability of the method over time.

Sensitivity is assessed by calculating the limit of detection (LOD) (signal-to-noise (S/N) of 3), ranging from 0.6-1.5 $\mu\text{g L}^{-1}$, and limit of quantification (LOQ) (S/N of 10), spanning 2.0-5.0 $\mu\text{g L}^{-1}$ (Table 1). These results validate the trace detection and quantitation capabilities of the proposed method with high accuracy and precision.

Real tea sample analysis

To demonstrate its applicability, the proposed methodology was applied to detect benzoylurea pesticide vestiges in three veritable tea samples: two commercial teas (green tea and oolong tea) and one tea beverage (purchased from a local market). We investigated its practical effectiveness in authentic settings by administering our tactic to bona fide tea preparations. The benzoylurea insecticide content in three tea brews was beneath the detection ceiling (Table 3). When heightened at three plateaus (15, 100, and 200 $\mu\text{g L}^{-1}$), satisfactory recoveries (74.9-94.0%) were attained, accompanied by low RSDs (0.51-9.0%). Figure 6 indicates that the detection is extensively impervious to matrix interference. These results suggest that the proposed method can effectively determine benzoylurea insecticides in authentic tea infusion samples.

All adsorption experiments in this study were performed using the same batch of $\text{SiO}_2/\text{PAMAM-G3}$ to establish its performance metrics. Batch-to-batch reproducibility assessment is one of the most important aspects for the practical applicability of our sorbent. Systematic production under the same synthesis conditions to analyze adsorption behavior homogeneity will be further researched systematically. A standardized synthesis protocol will be developed and implemented with rigorous quality control measures aimed at reducing batch variation. This will include complete batch characterization and thorough comparison of their adsorption efficiencies to ensure that all batches meet predetermined performance criteria.

Table 1. Analytical parameters of the method in tea samples with $\text{SiO}_2/\text{PAMAM-G3}$

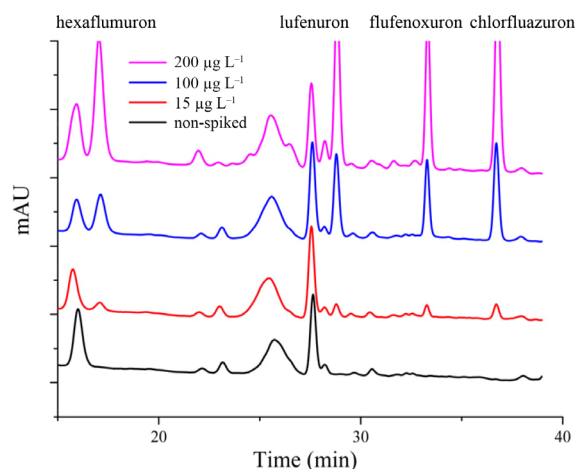
Analyte	Linear equation	R ²	R / %	Linear range / ($\mu\text{g L}^{-1}$)	LOD (n = 3) / ($\mu\text{g L}^{-1}$)	LOQ (n = 3) / ($\mu\text{g L}^{-1}$)
Hexaflumuron	$y = 1.4413x + 12.47$	0.9994	81.2	2-500	0.6	2.0
Lufenuron	$y = 2.0392x - 0.5383$	0.9994	86.0	2-500	0.6	2.0
Flufenoxuron	$y = 1.5871x - 0.8608$	0.9998	89.3	5-500	1.5	5.0
Chlorfluazuron	$y = 2.3622x + 3.0447$	0.9998	96.0	2-500	0.5	2.0

R²: adjusted coefficient of determination; R: recovery for the analytes; LOD: limit of detection; LOQ: limit of quantification; n: number of replicates; PAMAM-G3: polyamidoamine 3rd generation.

Table 2. Reproducibility parameters of the proposed method

Analyte	Intra-day RSD (n = 5) / %	Inter-day RSD (n = 3) / %	Batch to batch RSD (n = 5) / %
Hexaflumuron	2.8	2.7	2.2
Lufenuron	2.2	2.8	0.14
Flufenoxuron	1.7	2.0	0.22
Chlorfluazuron	1.4	3.9	0.39

RSD: relative standard deviation; n: number of replicates.

**Figure 6.** High-performance liquid chromatography (HPLC) chromatograms of the analytes at the detection wavelength of 220 nm.**Table 3.** Results of the determination of 4 benzoylureas in different real tea samples

Analyte	Spiked concentration / ($\mu\text{g L}^{-1}$)	Tea drink		Green tea		Oolong tea	
		R / %	RSD / %	R / %	RSD / %	R / %	RSD / %
Hexaflumuron	0	ND	–	ND	–	ND	–
	15	76.1	2.6	86.7	4.5	78.1	2.7
	100	77.2	3.1	82.7	0.76	75.9	1.3
	200	80.1	4.1	78.7	0.55	74.9	1.0
Lufenuron	0	ND	–	ND	–	ND	–
	15	80.7	6.4	84.4	3.0	77.3	3.0
	100	79.5	6.1	84.8	1.5	79.4	2.8
	200	79.9	3.8	78.7	0.51	78.8	2.5
Flufenoxuron	0	ND	–	ND	–	ND	–
	15	85.4	9.0	80.0	4.9	82.1	3.3
	100	85.1	3.2	88.3	1.0	82.3	3.2
	200	83.2	2.6	78.2	1.5	79.5	3.1
Chlorfluazuron	0	ND	–	ND	–	ND	–
	15	89.6	4.4	90.1	4.8	89.3	5.7
	100	87.2	1.6	90.1	0.67	89.7	0.71
	200	91.5	2.9	82.3	1.4	94.0	0.86

R: recovery for the analytes; RSD: relative standard deviation; ND: not detected.

Comparison with other methods

Our benchmarking elucidated consistent DSPE efficiencies, reducing processing time to 9 min *versus* the typically needed 30 min. This coincides with curtailed sample volumes, requiring merely 8 mL, contrasting with the 50 mL requirements of SPE. Table 4 summarizes statistics, including the limit of detection (LOD), sample quantity, and experimental time. Comparable techniques rival analytical performance within a wide 2-500 $\mu\text{g L}^{-1}$ linear dynamic range. The protocol also minimizes sorbent usage to 30 mg, substantially lower than the 100 mg demands imposed by nanotube-based methods. LODs in the range of 0.5-1.5 $\mu\text{g L}^{-1}$ demonstrate on-par sensitivity with leading protocols.

Conclusions

This work presents a dispersive solid phase microextraction technique employing tailored polyamidoamine dendrimer-grafted silica nanoparticles to selectively extract trace benzoylurea insecticide residues from intricate green tea infusion matrices. $\text{SiO}_2/\text{PAMAM-G3}$ nanocomposite synthesis, functionalization, and tailored structure are meticulously validated by FTIR and electron microscopy (SEM and TEM). Method optimizations afford excellent linearity over a broad dynamic range

Table 4. The comparison of the proposed method to the existing methods for determination of benzoylureas in different samples

Method	Sample	Sample volume / mL	time / min	Linearity range / ($\mu\text{g L}^{-1}$)	Extraction solvent or sorbent consumption	LOD / ($\mu\text{g L}^{-1}$)	Reference
DLLME-HPLC-UV	water and tea drinks	15	10	2-500	40 mg [N_{8881}]Cl	0.29-0.59	38
SPE-LC-MS/MS	oolong tea	50	30	5-50	30 mL dichloromethane	0.03-1.00	4
FDME-HPLC	peach juice	15	25	10-10000	8 μL 1-dodecanol	5.0-10.0	39
ISFME-DMSPE-HPLC	water	8	5	2-300	15 μL [HMIM]Cl + 235 μL LiNTf ₂ + 3 mg Fe ₃ O ₄ /nSiO ₂ /mSiO ₂	0.67-1.46	40
SPE-HPLC-DAD	water	50	54	0.2-40	100 mg TiO ₂ nanotube	0.062-0.21	41
DMSPE-HPLC	wea infusion	8	9	2-500	30 mg SiO ₂ /PAMAM-G3	0.5-1.5	this work

LOD: limit of detection; DLLME: dispersive liquid-liquid microextraction; HPLC-UV: high performance liquid chromatography with ultraviolet detector; SPE-LC-MS/MS: solid phase extraction-liquid chromatography tandem mass spectrometry; FDME: floated organic drop microextraction; ISFME: *in situ* solvent formation microextraction; DMSPE: dispersive micro-solid-phase extraction; HPLC: high performance liquid chromatography; SPE: solid phase extraction; DAD: diode array detection; [HMIM]Cl: 1-hexyl-3-methylimidazolium chloride; LiNTf₂: bis(trifluoromethane)sulfonimide lithium salt; [N_{8881}]Cl: methyl trioctyl ammonium chloride; PAMAM-G3: polyamidoamine 3rd generation.

down to environmentally relevant concentrations and the low limits of detection and quantification. Outstanding accuracy and precision are realized through consistent near-complete recoveries and negligible intra- and inter-day relative standard deviations. Clean extractions from commercial tea samples under stringent regulatory limits further verify the applicability for real-world samples. Additionally, practical enhancements like reduced solvent utilization reflect green chemistry motivations. This nano-engineered sorbent strategy significantly advances analytical capabilities, enabling sensitive, efficient, robust insecticide quantification. The universal merits of rational dendrimer nanocomposite design signify tremendous untapped opportunities for specialized extractions by judiciously tailoring building block attributes in the future.

Acknowledgments

This work was supported by the National Natural Science Foundation of China (project No. 21677174, 21277172).

We would like to thank MogoEdit for its English editing during the preparation of this manuscript.

Author Contributions

Yanchao Zhang was responsible for experiments and writing; Xiaoyan Cui and Xiwen Lin for writing; Yiduo Mi and Yumei Yan for assisting the experiments; Xiaoyang Liu and Keren Jiao for collecting and collating the sample data; Haixiang Gao, Runhua Lu and Wenfeng Zhou for supervision. All the authors discussed the results and commented on the manuscript.

References

- Hsiao, Y. L.; Ho, W. H.; Yen, J. H.; *Chemosphere* **2013**, *90*, 380. [Crossref]
- Liu, H. G.; Zhao, M. R.; Zhang, C.; Ma, Y.; Liu, W. P.; *Toxicology* **2008**, *253*, 89. [Crossref]
- Matsumura, F.; *Pestic. Biochem. Physiol.* **2010**, *97*, 133. [Crossref]
- Chen, L.; Chen, J. F.; Guo, Y.; Li, J. R.; Yang, Y. Q.; Xu, L. J.; Fu, F. F.; *Food Chem.* **2014**, *143*, 405. [Crossref]
- Nougadère, A.; Reninger, J. C.; Volatier, J. L.; Leblanc, J. C.; *Food Chem. Toxicol.* **2011**, *49*, 1484. [Crossref]
- Khan, N.; Mukhtar, H.; *Life Sci.* **2007**, *81*, 519. [Crossref]
- Huang, Y. S.; Shi, T.; Luo, X.; Xiong, H. L.; Min, F. F.; Chen, Y.; Nie, S. P.; Xie, M. Y.; *Food Chem.* **2019**, *275*, 255. [Crossref]
- Nie, S. P.; Xie, M. Y.; *Food Hydrocolloids* **2011**, *25*, 144. [Crossref]
- Cabrera, C.; Artacho, R.; Giménez, R.; *J. Am. Coll. Nutr.* **2006**, *25*, 79. [Crossref]
- Wang, Y. D.; Fu, Y. W.; Wang, Y. Y.; Lu, Q.; Ruan, H. N.; Luo, J. Y.; Yang, M. H.; *Food Chem.: X* **2022**, *15*, 100375. [Crossref]
- Khatibi, S. A.; Hamidi, S.; Siahi-Shadbad, M. R.; *Crit. Rev. Anal. Chem.* **2022**, *52*, 327. [Crossref]
- Dias, F. D.; Meira, L. A.; Carneiro, C. N.; Santos, L.; Guimarães, L. B.; Coelho, N. M. M.; Coelho, L. M.; Alves, V. N.; *TrAC, Trends Anal. Chem.* **2023**, *158*, 116891. [Crossref]
- Samadifar, M.; Yamini, Y.; Khataei, M. M.; Shirani, M.; *J. Chromatogr. A* **2023**, *1706*, 464227. [Crossref]
- Lai, H. S.; Yu, Z. N.; Li, G. K.; Zhang, Z. M.; *J. Chromatogr. A* **2022**, *1675*, 463181. [Crossref]
- Grecco, C. F.; de Souza, I. D.; Oliveira, I. G. C.; Queiroz, M. E. C.; *Separations* **2022**, *9*, 394. [Crossref]

16. Kataoka, H.; *J. Chromatogr. A* **2021**, *1636*, 461787. [Crossref]
17. Souza, I. D.; Oliveira, I. G. C.; Queiroz, M. E. C.; *Anal. Chim. Acta* **2021**, *1165*, 238110. [Crossref]
18. Jayasinghe, T. M.; Moreda-Piñeiro, A.; *Separations* **2021**, *8*, 99. [Crossref]
19. Dugheri, S.; Marrubini, G.; Mucci, N.; Cappelli, G.; Bonari, A.; Pompilio, I.; Trevisani, L.; Arcangeli, G.; *Acta Chromatogr.* **2021**, *33*, 99. [Crossref]
20. Sajid, M.; *TrAC, Trends Anal. Chem.* **2018**, *98*, 114. [Crossref]
21. Faraji, M.; Yamini, Y.; Gholami, M.; *Chromatographia* **2019**, *82*, 1207. [Crossref]
22. Lyu, Z. B.; Ding, L.; Dhumal, D.; Huang, A. Y.; Kao, C. L.; Peng, L. In *Dendrimer Chemistry: Synthetic Approaches Towards Complex Architectures*; Malkoch, M.; Gallego, S. G., eds.; Royal Society of Chemistry: London, 2020, p. 85.
23. Lotfi, R.; Hayati, B.; Rahimi, S.; Shekarchi, A. A.; Mahmoodi, N. M.; Bagheri, A.; *Microchem. J.* **2019**, *146*, 1150. [Crossref]
24. Patle, R. Y.; Meshram, J. S.; *React. Chem. Eng.* **2022**, *7*, 9. [Crossref]
25. Sajid, M.; Basheer, C.; *TrAC, Trends Anal. Chem.* **2016**, *75*, 174. [Crossref]
26. Kabir, A.; Hamlet, C.; Yoo, K. S.; Newkome, G. R.; Malik, A.; *J. Chromatogr. A* **2004**, *1034*, 1. [Crossref]
27. Shirani, M.; Faraji, M.; Rashidi, H. N.; Akbari-Adergani, B.; Sepahi, S.; *J. Food Sci. Technol.* **2023**, *60*, 2802. [Crossref]
28. General Administration of Quality Supervision, Inspection and Quarantine (AQSIQ) and the Standardization Administration of China (SAC); *Methodology of Sensory Evaluation of Tea GB/T 23776-2009*, China Standard Publishing House: Beijing, 2009 (in Chinese).
29. Izadi, M.; Mardani, H.; Roghani-Mamaqani, H.; Salami-Kalajahi, M.; *Bull. Mater. Sci.* **2021**, *44*, 199. [Crossref]
30. Geitner, N. K.; Zhao, W. L.; Ding, F.; Chen, W.; Wiesner, M. R.; *Environ. Sci. Technol.* **2017**, *51*, 8396. [Crossref]
31. Zhou, Q. X.; Wu, Y. L.; Sun, Y.; Sheng, X. Y.; Tong, Y. Y.; Guo, J. H.; Zhou, B. Y.; Zhao, J. Y.; *J. Environ. Sci.* **2021**, *102*, 64. [Crossref]
32. Shen, Y.; Chen, B.; van Beek, T. A.; *Green Chem.* **2015**, *17*, 4073. [Crossref]
33. Cameo Chemicals, <https://cameochemicals.noaa.gov/>, accessed in July 2024.
34. Funari, C. S.; Carneiro, R. L.; Khandagale, M. M.; Cavaleiro, A. J.; Hilder, E. F.; *J. Sep. Sci.* **2015**, *38*, 1458. [Crossref]
35. Shirani, M.; Parandi, E.; Nodeh, H. R.; Akbari-Adergani, B.; Shahdadi, F.; *Food Chem.* **2022**, *373*, 131421. [Crossref]
36. Shirani, M.; Aslani, A.; Ansari, F.; Parandi, E.; Nodeh, H. R.; Jahanmard, E.; *Microchem. J.* **2023**, *189*, 108507. [Crossref]
37. Seyed, Z.; Esmailipour, O.; Shirani, M.; Nodeh, H. R.; Mazhari, M.; *Food Addit. Contam.: Part A* **2022**, *39*, 1521. [Crossref]
38. Wang, H. Z.; Hu, L.; Li, W. Z.; Yang, X. L.; Lu, R. H.; Zhang, S. B.; Zhou, W. F.; Gao, H. X.; Li, J.; *Talanta* **2017**, *162*, 625. [Crossref]
39. Zhou, J.; Liu, R.; Song, G.; Zhang, M.; *Anal. Lett.* **2009**, *42*, 1805. [Crossref]
40. Zhang, Y.; Yang, X. L.; Wang, J. K.; Zhou, W. F.; Lu, R. H.; Gao, H. X.; Zhang, S. B.; *J. Sep. Sci.* **2017**, *40*, 442. [Crossref]
41. Huang, Y.; Zhou, Q.; Xie, G.; Liu, H.; Lin, H.; *Microchim. Acta* **2011**, *172*, 109. [Crossref]

Submitted: March 28, 2024

Published online: August 6, 2024